**Appl. Chem. Eng.,** Vol. 31, No. 5, October 2020, 495-501
https://doi.org/10.14478/ace.2020.1058

Article

# Adsorptive Removal of Phosphate Ions from Aqueous Solutions using Zirconium Fumarate

**Phani B. S. Rallapalli and Jeong Hyub Ha†**

*Department of Integrated Environmental Systems, Pyeongtaek University, Pyeongtaek 17869, Korea*
*(Received July 27, 2020; Revised August 17, 2020; Accepted August 17, 2020)*

**Abstract**

In this study, zirconium fumarate of metal-organic framework (MOF-801) was solvothermally synthesized at 130 ℃ and characterized through powder X-ray diffraction (PXRD) analyses and porosity measurements from $N_2$ sorption isotherms at 77 K. The ability of MOF-801 to act as an adsorbent for the phosphate removal from aqueous solutions at 25 ℃ was investigated. The phosphate removal efficiency (PRE) obtained by 0.05 g/L adsorbent dose at an initial phosphate concentration of 60 ppm after 3 h was 72.47%, whereas at 5 and 20 ppm, the PRE was determined to be 100% and 89.88%, respectively, after 30 min for the same adsorbent dose. Brunauer-Emmett-Teller (BET) surface area and pore volume of the bare MOF-801 sample were 478.25 $m^2/g$ and 0.52 $cm^3/g$, respectively, whereas after phosphate adsorption (at an initial concentration of 60 ppm, 3 h), the BET surface area and pore volume were reduced to 331.66 $m^2/g$ and 0.39 $cm^3/g$, respectively. The experimental data of kinetic (measured at initial concentrations of 5, 20 and 60 ppm) and isotherm measurements followed the pseudo-second-order kinetic equation and the Freundlich isotherm model, respectively. This study demonstrates that MOF-801 is a promising material for the removal of phosphate from aqueous solutions.

***Keywords***: *Eutrophication, Phosphate removal, Metal-organic frameworks, Kinetics, Chemisorption*

## 1. Introduction

Phosphate is one of the most well-known compounds associated with wastewater streams and is a major nutrient that contributes toward eutrophication, a universal pollution problem faced by fresh water ecosystems. The industrial and municipal effluent streams, containing phosphate, are usually released into water bodies. The accumulated phosphate in the surface water, although having a low concentration, induces algae and plant growth. It depletes the quantity of dissolved oxygen, which, in turn, may lead to fish kills and loss of other aquatic life. This disturbs the balance in the aquatic ecosystem and deteriorates the quality of water. Therefore, it is essential to reduce phosphate levels in the wastewater streams before they are discharged into the fresh water ecosystems[1].

To reduce phosphate levels in wastewater streams, several biological, chemical, physical, and physicochemical methods have been employed [2,3]. The adsorption process is more promising in comparison to other procedures owing to its ease of operation, simplicity of design, and economics, provided that low-cost sorbents are used.[4]. Several adsorbents such as metal oxides and hydroxides[5,6], layered double hydroxide (LDH)[7], clay materials[8], industrial by-products such as fly ash[9], metal loaded carbon[10], anion exchange resins[11], and metal loaded silica[12] have been studied for phosphate adsorption.

Metal-Organic Frameworks (MOFs), formed by a combination of metallic clusters with organic ligands, have attracted considerable attention as novel adsorbents for catalysis, gas storage and separation, and drug delivery owing to their large surface areas and pore volume[13]. Recently, MOFs have been widely studied for applications in selective adsorption and removal of toxic dyes[14], pharmaceuticals[15], nitrogen compounds[16], sulfur compounds[17], and heavy metal ions[18].

A major disadvantage of many MOF materials is their limited stability with regard to temperature fluctuations, and a high reactivity with water, oxygen, along with other chemicals. For example, some $Zn^{2+}$-based MOFs, including MOF-5, are liable to hydrolysis when stored at ambient temperature[19]. Very few reports are available on phosphate adsorption using zirconium-based MOFs in the literature. However, recently, $Zr^{4+}$-based MOFs have attracted researchers' interest owing to their thermal stability and non-reactivity with water. Moreover, phosphate adsorption from water and urine via zirconium-based MOFs, UIO-66, and UIO-66-$NH_2$[20], as well as the adsorption of glyphosate [*N*-(phosphonomethyl) glycine], an organic phosphate, via a zirconium-based MOF (UIO-67) have been reported[21].

In the present study, MOF-801 (zirconium fumarate) was solvothermally synthesized and characterized by PXRD and $N_2$ sorption isotherms measured at 77 K. The ability of MOF-801 to adsorb for phosphate from aqueous solutions at 25 ℃ was investigated. The parameters affecting the phosphate removal efficiency (PRE) such as adsorbent dosage, contact time and initial phosphate concentration were evaluated. In addition, the experimental data were examined using a nonlinear isotherm model and the pseudo-first-order and pseudo-second-order kinetic equation.

† Corresponding Author: Pyeongtaek University,
Department of Integrated Environmental Systems, Pyeongtaek 17869, Korea
Tel: +82-31-659-8309 e-mail: jhha@ptu.ac.kr

pISSN: 1225-0112 eISSN: 2288-4505 

## 2. Materials & Methods

### 2.1. Materials

Zirconium (IV) oxychloride octahydrate ($ZrOCl_2 \cdot 8H_2O$, 99%), fumaric acid ($C_4O_4H_4$, extra pure), formic acid (HCOOH, 85%, extra pure), dimethylformamide (DMF, guaranteed reagent) potassium phosphate monobasic ($KH_2PO_4$, 99%), L(+)-ascorbic acid (Special grade, 99.5%), and ammonium molybdate tetrahydrate were purchased from Samchun Chemicals Ltd., South Korea. Potassium antimonyl tartarate sesquihydrate (> 99%) was purchased from Acros Organics, USA.

### 2.2 Methods

2.2.1. Preparation of MOF-801

The procedure was adopted from Ke *et al.*[22]. A solution was created by dissolving 3.2 g of $ZrOCl_2 \cdot 8H_2O$ and 1.16 g of fumaric acid in 54 mL DMF-14 mL formic acid solution. Afterwards, the clear solution was put into an autoclave for crystallization at 130 ℃ for 6 h. After reaction, the obtained product was filtered and washed with water and ethanol, and then dried overnight at 100 ℃.

2.2.2. Instrumentation

The powder X-ray diffraction (PXRD) patterns for MOF-801 were measured at ambient temperature by a PHILIPS X'pert MPD diffractometer in the $2\theta$ range of 2°~60°, at a scan speed of 0.1 °/s using CuK$\alpha$1 ($\lambda$ = 1.54056 Å) radiation. The BET surface area, pore volume, and pore diameter of the MOF-801 were determined in a static volumetric gas adsorption system (Micromeritics Instrument Corporation, USA, model ASAP 2020) using the $N_2$ adsorption-desorption isotherm at 77.4 K up to a relative pressure of 1 bar. The BET equation and the single point adsorption methods were employed for estimating the surface area and the pore volume, respectively. Fourier transform infrared (FTIR) spectra were collected on a Jasco FTIR-6100 spectrometer at room temperature with 1.0 cm-1 resolution. The phosphate concentration was measured by the molybdenum blue method using Orion Aquamate-8000, which is a UV-VIS spectrophotometer (Thermo Fischer Inc., USA).

2.2.3. Phosphate Adsorption measurements

2.2.3.1. Effect of initial phosphate concentration, contact time and adsorbent dose

To determine the effect of initial phosphate concentration on phosphate removal, 50 mg of MOF-801 sample was taken in to 100 mL phosphate solution. The initial concentrations of the phosphate solutions were in the range of 5~80 ppm. The suspensions were placed on a shaker and stirred for 3 h. The suspensions were then filtered, and the residual phosphate concentration was measured.

The effect of contact time on phosphate removal was also examined. For this study, 50 mg of MOF-801 sample was taken in to 100 mL of three different phosphate solutions with initial concentrations of 5, 20 and 60 ppm. The suspensions were placed on a shaker and stirred for 180 min. The suspensions were taken out from the shaker at specified time intervals and filtered. This filtrate was diluted to 10 times and the residual phosphate concentration was measured.

The adsorbent dosage on phosphate removal was investigated at three different initial phosphate concentrations of 5, 20 and 60 ppm. Various doses of MOF-801 sample, ranging between 0.025~0.075 mg, were added to 100 mL phosphate solutions. The suspensions were placed on a shaker and stirred for 3 h. After completion of the experiment, the suspensions were filtered and the residual phosphate concentrations were measured.

2.2.3.2. Phosphate adsorption studies using real wastewater

Influent wastewater was collected from the Poseung wastewater treatment plants, located in Pyeongtaek city. Before phosphate adsorption experiments, the wastewater was filtered and autoclaved at 120 ℃ for 3 h. Various doses of MOF-801 sample between 0.025-0.075 mg, were added to a 100 mL sample solution and the rest of experiments were carried out as mentioned in Section 2.2.3.1.

2.2.3.3. Determination of phosphate concentration

The phosphate concentration was measured by the molybdenum blue method using the Orion Aquamate-8000. The percentage of PRE was calculated by the following equation:

$$\text{PRE } (\%) = \frac{(C_o - C_e)}{C_o} \times 100 \quad (1)$$

The phosphate removal capacity (PRC) at equilibrium was calculated by the following equation:

$$\text{PRC (mg/g)} = (C_o - C_e) \times \frac{V}{m} \quad (2)$$

where $C_o$ and $C_e$ are the initial and equilibrium concentrations of phosphate ion in mg/L, $V$ is the volume of the sample solution in L, and $m$ is the dosage of adsorbent in grams.

## 3. Results and Discussion

### 3.1. Characterization

Initially, the synthesis of MOF-801 was reported by using zirconium tetrachloride and fumaric acid as the metal and organic linker precursors, respectively, with formic acid as the modulator in this synthesis[19]. Later, the MOF-801 was produced using zirconium oxychloride as the metal precursor[22]. It is composed of 12-connected Zr-based clusters[$Zr_6O_4(OH)_4(\text{-}COO)_{12}$], joined by fumarate linkers into a three-dimensional, extended microporous framework of face-centered cubic topology[19]. The PXRD pattern of MOF-801 sample was examined (data not shown) and was found to match well with the previous reports[19,22]. In addition, the $N_2$ sorption isotherms were examined (data not shown). The isotherms of Type-1 showed that the MOF-801 is a microporous material which matched well with the previous reports[19,22]. The BET surface area and pore volume of the bare MOF-801 sample were measured to be 478.25 $m^2/g$ and 0.52 $cm^3/g$,

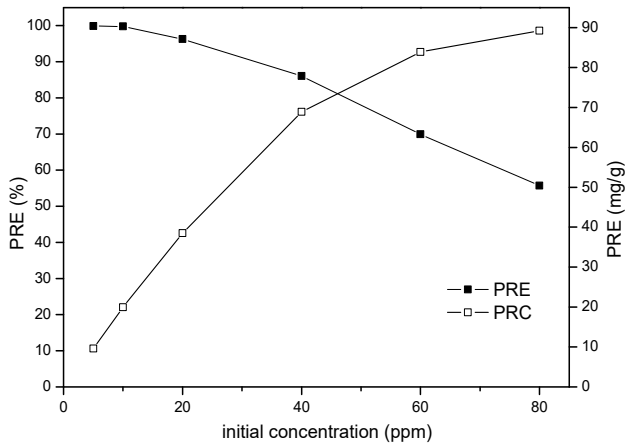


**Figure 1. Effect of initial concentration on PRE (%) and PRC (mg/g). At adsorbent dosage: 0.05 g, volume: 100 mL, adsorption time: 3 h, adsorption temperature: 25 ℃.**

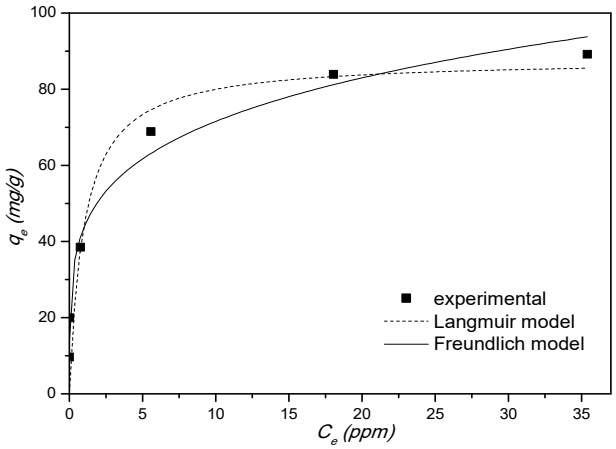


**Figure 2. Experimental and nonlinear curve fittings for the Langmuir and the Freundlich isotherm models.**

respectively.

### 3.2. Effect of initial concentration on phosphate removal

The effect of changing the initial phosphate concentration (i.e., 5, 10, 20, 40, 60 and 80 ppm) on PRE (%) and PRC were studied while keeping the MOF-801 amount constant and the results are shown in Figure 1. The PRE (%) gradually decreased from 96.37% to 55.75% as the initial phosphate concentration increased from 5 to 80 ppm. On the other hand, an increase in the removal capacity from 9.6~89.20 (mg/g) was observed with an increase in the initial phosphate concentration from 5 to 80 ppm. The decrease in the PRE with increasing initial phosphate concentration can be attributed to the fact that at constant adsorbent dosage, the total number of available adsorption sites present in the MOF-801 surface are fixed. This implies that a certain amount of MOF-801 adsorbs almost the same amount of phosphate ions, resulting in a decrease in the PRE (%). However, the adsorption capacity at equilibrium increased with an increase in the initial phosphate ion concentration. The initial concentration of the phosphate ions provides the necessary driving force to overcome the mass transfer resistance and enhances the interaction between the phosphate ions in the aqueous phase and the MOF-801 surface. Therefore, a higher initial concentration of phosphate ions results in an increased rate of adsorption. Similar results were reported by Das *et al.*[23]. The experimental data was fitted to the nonlinear Langmuir and Freundlich isotherm models given by the equations (3) and (4), respectively[24]:

$$q_e = \frac{bq_m C_e}{1+bC_e} \tag{3}$$

$$q_e = kC_e^{1/n} \tag{4}$$

where $C_e$ represents the equilibrium concentration of the phosphate ions, $q_e$ (mg/g) represents the amount of phosphate adsorbed per unit mass of adsorbent at equilibrium, $q_m$ (mg/g) is the Langmuir constant that represents maximum adsorption capacity by assuming a monolayer coverage of adsorbate over a homogenous adsorbent surface, $b$ is a kinetic parameter representing the adsorption energy of the adsorbent for the adsorbate phosphate, $k$ (mg/g) is the Freundlich constant related to the adsorption capacity, and $1/n$ is an empirical parameter related to adsorption intensity or surface heterogeneity. The results are shown in Figure 2.

As shown in Figure 2, the Freundlich model ($R^2$ = 0.9819) was a considerably better fit than the Langmuir model ($R^2$ = 0.8996), which suggests that the adsorption of the phosphate anions occurred on a heterogeneous surface.

### 3.3. Effect of contact time on phosphate removal

The PRE (%) was considerably higher for initial phosphate concentrations in the range of 5~20 ppm (99.9~97.7%). Increasing the initial phosphate concentrations over 60 ppm resulted in the lowering of PRE to below 60%. Hence, three different phosphate concentrations, 10, 20 and 60 ppm were chosen as low, medium and high phosphate concentrations, respectively, and the effect of contact time on PRE (%) and PRC were studied using them. The effect of contact time on PRE (%) was studied for up to 150 min on the three different initial phosphate concentrations (5, 20 and 60 ppm) and the results are illustrated in Figure 3. In the case of 5 ppm initial phosphate concentration, 100% PRE was obtained within 30 min. The PRE (%) at 5 and 15 min were further measured for the 5 ppm initial phosphate concentration and were observed to be 94.36% and 98.35%, respectively (these values are not shown in Figure 3 for simplicity). More than 90% of the phosphate ions were removed within 5 min in case of the 5 ppm sample, whereas for 20 and 60 ppm samples, the PRE (%) increased with the contact time and attained equilibrium after 120 min. Furthermore, no significant change in the rate of adsorption was observed until 150 min. The PRE (%) at 150 min were calculated as 97.72% and 67.21% for the 20 and 60 ppm samples, respectively. Beyond 30 min of contact time, the amount of phosphate adsorbed on the MOF-801 sample includes diffusion through the fluid layer around the adsorbent particle

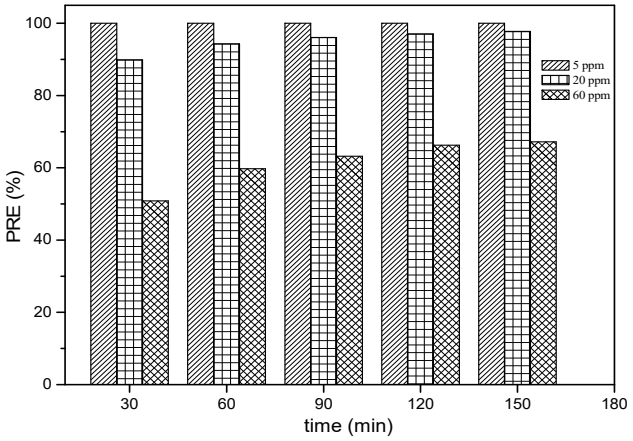


**Figure 3. Effect of contact time on PRE (%) and PRC (mg/g). At initial phosphate concentrations: 5, 20 and 60 ppm, volume: 100 mL, adsorbent dosage: 0.05 g, adsorption temperature: 25 ℃.**

and through the pores to the internal adsorption sites. In the initial stages of adsorption of phosphate, the concentration gradient between the layer and the available pore sites is large, and hence, the rate of adsorption is high. The rate of adsorption decreased in the later stages of the adsorption probably owing to reduced pore diffusion of the solute ion into the bulk of the adsorbent[25], and it plateaued at about 120 min.

Estimation of adsorption kinetics provides information about the sorption rates and the sorption mechanism. The experimental adsorption kinetics data was fitted to the nonlinear pseudo-first-order and pseudo-second-order kinetic models according to equations (5) and (6), respectively[26]:

$$q_t = q_e\left(1-e^{-k_1 t}\right) \tag{5}$$

$$q_t = \frac{q_e^2 k_2 t}{q_e k_2 t+1} \tag{6}$$

where $q_e$ (mg/g) and $q_t$ (mg/g) are the amount of phosphate ions adsorbed per unit mass of the adsorbent at equilibrium and at any time $t$ (min), respectively; $k_1$ (per min) is the rate constant of the pseudo-first-order kinetic model and $k_2$ (g/mg per min) is the rate constant for the pseudo-second-order kinetic model. The kinetic model fittings for the 60 ppm sample are shown in Figure 4.

The experimental data corresponded well to the pseudo-second-order kinetic model ($R^2$ = 0.9941) compared to the pseudo-first-order kinetic model ($R^2$ = 0.9216). The calculated removal capacity at 150 min was 80.60 mg/g which is close to the experimental removal capacity (80.65 mg/g). The phosphate adsorption capacities of various adsorbents are given in Table 1. Zr-fumarate shows a higher phosphate adsorption capacity compared to the modified zeolites, silica, and graphene oxide but a lower adsorption capacity than the Fe-Zr binary oxide and the amorphous zirconium nano particles[27-34]. According to the kinetic model, the rate-limiting step here involves surface adsorption, a chemisorption

**Table 1. Phosphate Adsorption Capacities of Various Adsorbents**

| Adsorbent | Adsorption capacity (mg/g) | Reference |
|---|---|---|
| Fe-Zr binary oxide | 102.30 | [27] |
| Zr modified zeolite | 10.20 | [28] |
| Mesoporous zirconia | 29.71 | [29] |
| Zr-SBA-15 | 13.77 | [30] |
| Am-$ZrO_2$ nanoparticles | 99.01 | [31] |
| Amorphous $Zr(OH)_2$ | 17.00 | [32] |
| Zr-Mg-Al | 30.00 | [33] |
| Go-Zr | 16.45 | [34] |
| Zr-fumarate | 80.6 | Present study |

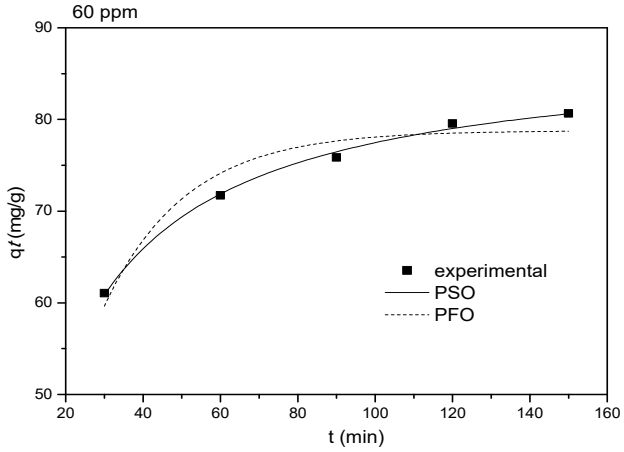


**Figure 4. Experimental and nonlinear curve fittings for the pseudo-first-order and pseudo-second-order kinetic models.**

process[28]. MOF-801 possesses plenty of hydroxyl groups that are present in the nodes of Zr (IV). These zirconium-bound hydroxyl groups in the nodes of the framework are expected to facilitate the adsorption of phosphate via the anion exchange property. Fluoride removal using MOF-801 via the exchange of zirconium-bound hydroxyl groups has been verified[22], and the experimental results in this study further confirmed that the phosphate removal on MOF-801 sample also follows chemisorption via the ligand exchange mechanism. The BET surface area and the pore volume of the MOF-801 sample were measured after phosphate adsorption (at an initial phosphate concentration of 60 ppm, after 3 h, without washing the sample) and they were observed to be 331.66 $m^2$/g and 0.39 $cm^3$/g, respectively. Hence, a 30.65% reduction was observed in the BET surface area after phosphate adsorption.

### 3.4. Effect of Adsorbent dosage on phosphate removal

Figure 5 illustrates the effect of adsorbent dosage on PRE (%) at three different initial phosphate concentrations: 5, 20 and 60 ppm. 100% PRE was observed in the case of the 5 ppm solution. In contrast, a constant increase of the PRE (%) was observed in the case of the 60 ppm solution. The PRE obtained by a 0.075 mg adsorbent dose for the 5, 20 and 60 ppm initial phosphate concentration samples were

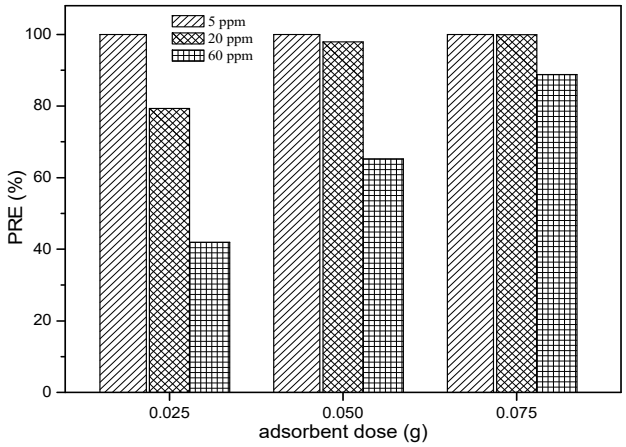


**Figure 5. Effect of MOF-801 dosage on the PRE (%). At initial phosphate concentrations: 5, 20 and 60 ppm, volume: 100 mL, adsorption time: 3 h, adsorption temperature: 25 ℃.**

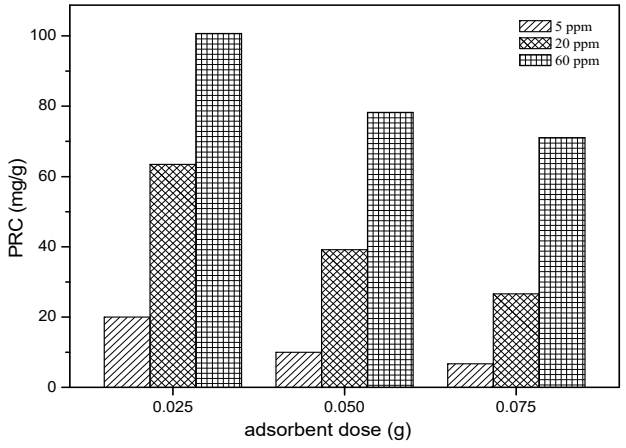


**Figure 6. Effect of MOF-801 dosage on PRC (mg/g). At initial phosphate concentrations: 5, 20 and 60 ppm, volume: 100 mL, adsorption time: 3 h, adsorption temperature: 25 ℃.**

100, 99.90, and 88.81%, respectively. Figure 6 illustrates the effect of adsorbent dosage on PRC (mg/g) at the three different initial phosphate concentration solutions: 5, 20 and 60 ppm. PRC decreased with an increase in the adsorbent dosage. This indicates that MOF-801 was not completely utilized under high dosage conditions. It is likely that during phosphate adsorption process, the hydroxyl groups bound to MOF-801 surface (Zr-OH) were discharged and they accumulated in the vicinity of the MOF-801 surface, repelling the other phosphate anions and decreasing the phosphate removal capacity. Similar results were reported by Dexin *et al.*[35].

### 3.5. Experimental results using wastewater samples

The initial phosphate ion concentration in the Poseung wastewater treatment plant of Pyeongtaek city was measured to be 15.01 ppm and the composition of raw wastewater was presented in Table 2. The phosphate adsorption experiments were conducted at three different adsorbent doses, 25, 50 and 75 mg, using 100 mL of wastewater samples.

**Table 2. Variations of Water Quality of Influent Wastewater in Poseung Wastewater Treatment Plant**

| Items | Units | Raw wastewater |
|---|---|---|
| BOD | mg/L | 89.9~99.2 |
| COD | mg/L | 87.9~100.9 |
| SS | mg/L | 100.3~119.5 |
| T-N | mg/L | 37.9~41.7 |
| T-P | mg/L | 4.5~15.3 |

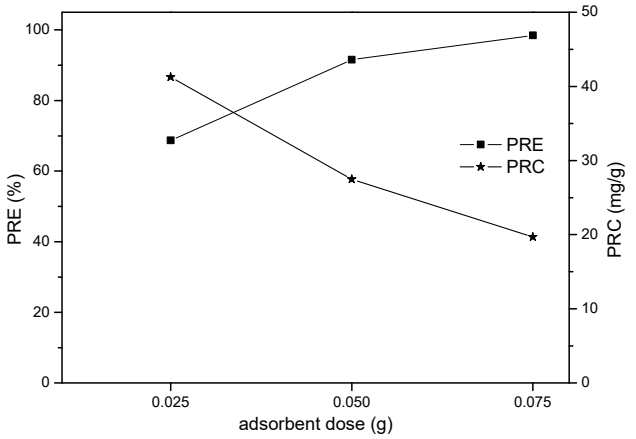


**Figure 7. Effect of MOF-801 dosage on PRE (%) and PRC (mg/g). At initial phosphate concentration of wastewater: 15.01 ppm, volume: 100 mL, adsorption time: 3 h, adsorption temperature: 25 ℃.**

Figure 7 illustrates the effect of the adsorbent dose on PRE (%) and PRC. The PRE (%) obtained for the 25, 50 and 75 mg dose was 68.7, 91.5, and 98.45%, respectively, whereas the PRC obtained was 41.24, 27.47 and 19.70 mg/g, respectively. A constant increase in the PRE (%) was observed with an increase in the adsorbent dose, whereas the PRC decreased with an increased the adsorbent dosages. These trends are similar to the previous results that were obtained for the 20 ppm initial phosphate concentration solution in Section 3.2.

## 4. Conclusions

The MOF-801 was prepared by solvothermal synthesis method and its ability to adsorb phosphate from aqueous solutions was investigated. The experimental data from kinetic (measured at initial concentrations of 5, 20 and 60 ppm) and isotherm measurements fitted well into the pseudo-second-order kinetic equation and the Freundlich isotherm model, respectively. These results suggest that phosphate removal was carried out via a chemisorption process and the adsorption occurred on a heterogeneous surface. The adsorption capacity of Zr-fumarate calculated from the PSO equation was found to be 80.6 mg/g, which is higher than that for the zirconium modified zeolites, silica, and graphene oxide. The Zr-fumarate removed more than 98% of the phosphate ions from the wastewater collected from the Poseung wastewater treatment plant, where the initial concentration of phosphate was 15.01 ppm. This study demonstrates that MOF-801 is a promising material

for removal of phosphate ion from aqueous solutions.

## Acknowledgements

This research was supported by the Basic Science Research Program through the National Research Foundation of Korea (NRF), funded by the Ministry of Education (2017R1D1A1B03033256).

## References

1. K. B. Biplob, I. Katsutoshi, N. G. Kedar, H. Hiroyuki, O. Keisuke, and K. Hidetaka, Removal and recovery of phosphorus from water by means of adsorption onto orange waste gel loaded with zirconium, *Bioresour. Technol.*, **99**, 8685-8690 (2008).
2. K. G. Ravindra, B. Sushmita, K. G. Pavan, and M. C. Chattopadhyaya, Remediation technologies for phosphate removal from wastewater: An overview. In J. A. Daniels (Ed), *Advances in Environmental Research*, Nova Science Publishers, Inc., **36**, 177-200 (2014).
3. T. B. Joshua, N. Edmond, D. O. Irina, M. Andrew, and W. G. David, A Review of phosphorus removal technologies and their applicability to small-scale domestic wastewater treatment systems, *Front. Environ. Sci.*, **6**, 1-15 (2018).
4. P. Loganathan, V. Saravanamuthu, J. Kandasamy, and S. B. Nanthi, Removal and recovery of phosphate from water using sorption, *Crit. Rev. Environ. Sci. Technol.*, **44**, 847-907 (2014).
5. R. Chitrakar, S. Tezuka, A. Sonoda, K. Sakane, K. Ooi, and T. Hirotsu, Selective adsorption of phosphate from sea water and wastewater by amorphous zirconium hydroxide, *J. Colloid Interface Sci.*, **297**, 426-433 (2006).
6. G. Zhang, H. Liu, R. Liu, and J. Qu, Removal of phosphate from water by a Fe-Mn binary oxide adsorbent, *J. Colloid Interface Sci.*, **335**, 168-174 (2009).
7. S. Karaca, A. Gurses, M. Ejder, and M. Acikyildiz, Adsorptive removal of phosphate from aqueous solutions using raw and calcined dolomite, *J. Hazard. Mater.*, **B128**, 273-279 (2006).
8. S. M. Ashekuzzaman and J. Jia-Qian, Study on the sorption-desorption-regeneration performance of Ca-, Mg- and CaMg-based layered double hydroxides for removing phosphate from water, *Chem. Eng. J.*, **246**, 97-105 (2014).
9. J. K. Edzwald, D. C. Toensing, and M. C. Y. Leung, Phosphate adsorption reactions with clay minerals, *Environ. Sci. Technol.*, **10**, 485-490 (1976).
10. X. Cui, X. Dai, K. Y. Khan, T. Li, X. Yang, and Z. He, Removal of phosphate from aqueous solution using magnesium-alginate/chitosan modified biochar microspheres derived from Thalia dealbata, *Bioresour. Technol.*, **218**, 1123-1132 (2016).
11. R. Awual, A. Jyo, S. A. El-Safty, M. Tamada, and N. Seka, A weak-fibrous anion exchanger effective for rapid phosphate removal from water, *J. Hazard. Mater.*, **188**, 164-171 (2011).
12. E. Ou, J. Zhou, S. Mao, J. Wang, F. Xia, and L. Min, Higly efficient removal of phosphate by lanthanum-doped mesoporous $SiO_2$, *Colloids Surf. A. Physicochem. Eng. Aspects*, **308**, 47-53 (2007).
13. H. Furukawa, K. E. Cordova, M. O'Keeffe, O. M. Yaghi, The chemistry and applications of metal-organic frameworks, *Science*, **341**, 974 (2013).
14. B. J. Yao, W. L. Jiang, Y. Dong, Z. X. Liu, and Y. B. Dong, Post-synthetic polymerization of UiO-66-$NH_2$ nanoparticles and polyurethane oligomer toward stand-alone membranes for dye removal and separation, *Chem. Eur. J.*, **22**, 10565-10571 (2016).
15. M. Wu, H. L. Ye, F. Q. Zhao, and B. Z. Zeng, High-quality metal-organic framework ZIF-8 membrane supported on electrodeposited ZnO/2-methylimidazole nanocomposite: Efficient adsorbent for the enrichment of acidic drugs, *Sci. Rep.*, **7**, 39778 (2017).
16. P. W. Seo, N. A. Khan, and S. H. Jhung, Removal of nitroimidazole antibiotics from water by adsorption over metal-organic frameworks modified with urea or melamine, *Chem. Eng. J.*, **315**, 92-100 (2017).
17. S. Aslam, F. Subhan, Z. F. Yan, U. J. Etim, and J. B. Zeng, Dispersion of nickel nanoparticles in the cages of metal-organic framework: An efficient sorbent for adsorptive removal of thiophene, *Chem. Eng. J.*, **315**, 469-480 (2017).
18. Z. Q. Xie, W. W. Xu, X. D. Cui, and Y. Wang, Recent progress in metal-organic frameworks and their derived nanostructures for energy and environmental applications, *Chem. Sus. Chem.*, **10**, 1645-1663 (2017).
19. G. Wißmann, A. Schaate, S. Lilienthal, I. Bremer, A. M. Schneider, and P. Behrens. Modulated synthesis of Zr-fumarate MOF, *Microporous Mesoporous Mater.*, **152**, 64-70 (2012).
20. K. Y. A. Lin, S. Y. Chen, and A. P. Jochems, Zirconium-based metal organic frameworks: Highly selective adsorbents for removal of phosphate from water and urine, *Mater. Chem. Phys.*, **160**, 168-176, (2015).
21. X. Zhu, B. Li, J. Yang, Y. Li, W. Zhao, J. Shi, and J. Gu, Effective adsorption and enhanced removal of organophosphorus pesticides from aqueous solution by Zr-based MOFs of UIO-67, *ACS Appl. Mater. Interfaces*, **7**, 223-231 (2015).
22. F. Ke, C. Peng, T. Zhang, M. Zhang, C. Zhou, H. Cai, J. Zhu, and X. Wan, Fumarate-based metal-organic frameworks as a new platform for highly selective removal of fluoride from brick tea, *Sci. Rep.*, **8**, 939 (2018).
23. J. Das, B. S. Patra, N. Baliarsingh, and K. M. Parida, Adsorption of phosphate by layered double hydroxides in aqueous solutions, *Appl. Clay Sci.*, **32**, 252-260 (2006).
24. D. Shilin, F. Dexin, P. Zishan, L. Bin, K. Li, W. Han, Z. Qian, S. Qiushi, and J. Fangying, Immobilization of powdery calcium silicate hydrate via PVA covalent cross-linking process for phosphorus removal, *Sci. Total Environ.*, **645**, 937-945 (2018).
25. M. Hamou, A. Hammou, A. Mustapha, and M. Hamid, Critical of linear and nonlinear equations of pseudo-first order and pseudo-second order kinetic models, *Karbala Int. J. Mod. Sci.*, **4**, 244-254 (2018).
26. R. Dariush, Pseudo-second-order kinetic equations for modeling adsorption systems for removal of lead ions using multi-walled carbon nanotube, *J. Nanostruct. Chem.*, **3**, 55-60 (2013).
27. Z. Ren, L. Shao, and G. Zhang, Adsorption of phosphate from aqueous solution using an iron-zirconium binary oxide sorbent, *Water, Air Soil Pollut.*, **223**, 4221-4231 (2012).
28 M. Yang, J. Lin, Y. Zhan, Z. Zhu, and H. Zhang, Immobilization of phosphorus from water and sediment using zirconium-modified zeolites, *Environ. Sci. Pollut. Res. Int.*, **22**, 3606-3619 (2015).
29. H. Liu, X. Sun, C. Yin, and C. Hu, Removal of phosphate by mesoporous ZrO2, *J. Hazard. Mater.*, **151**, 616-622 (2008).
30. Y. Tang, E. Zong, H. Wan, Z. Xu, S. Zheng, and D. Zhu, Zirconia functionalized SBA-15 as effective adsorbent for phosphate re-

moval, *Microporous Mesoporous Mater.*, **155**, 192-200 (2012).
31. Y. Su, H. Cui, Q. Li, S. Gao, and J. K. Shang, Strong adsorption of phosphate by amorphous zirconium oxide nanoparticles, *Water Res.*, **47**, 5018-5026 (2013).
32. R. Chitrakar, S. Tezuka, A. Sonoda, K. Sakane, K. Ooi, and T. Hirotsu, Selective adsorption of phosphate from seawater and wastewater by amorphous zirconium hydroxide. *J. Colloid Interface Sci.*, **297**, 426-433 (2006).
33. R. Chitrakar, S. Tezuka, A. Sonoda, K. Sakane, K. Ooi, and T. Hirotsu, Synthesis and phosphate uptake behavior of $Zr^{4+}$ incorporated MgAl-layered double hydroxides, *J. Colloid Interface Sci.*, **313**, 53-63 (2007).
34. E. Zong, D. Wei, H. Wan, S. Zheng, Z. Xu, and D. Zhu, Adsorptive removal of phosphate ions from aqueous solution using zirconia-functionalized graphite oxide, *Chem. Eng. J.*, **221**, 193-203, (2013).
35. F. Dexin, H. Liping, F. Zhuoyao, Z. Qian, S. Qiushi, L. Yimeng, X. Xiaoyi, and I. J. Fangy, Evaluation of porous calcium silicate hydrate derived from carbide slag for removing phosphate from wastewater, *Chem. Eng. J.*, **354**, 1-11 (2018).

**Authors**

Phani B. S. Rallapalli, Ph.D., Post-doc, Department of Integrated Environmental Systems, Pyeongtaek University, Pyeongtaek 17869, Korea; rphanirallapalli@gmail.com

Jeong Hyub Ha, Ph.D., Professor, Department of Integrated Environmental Systems, Pyeongtaek University, Pyeongtaek 17869, Korea; jhha @ptu.ac.kr